Experimental and Theoretical Studies of Isoprene Reaction with NO_3

Inseon Suh, Wenfang Lei, and Renyi Zhang*

Department of Atmospheric Sciences, Texas A&M University, College Station, Texas 77843

Received: February 15, 2001; In Final Form: April 20, 2001

The reaction of isoprene with nitrate radicals (NO_3) has been investigated using combined experimental and theoretical approaches. A fast-flow reactor coupled to chemical ionization mass spectrometry (CIMS) detection was used to measure the rate constant of the NO_3−isoprene reaction, yielding a value of $(7.3 \pm 0.2) \times 10^{-13}$ cm^3 $molecule^{-1}$ s^{-1} in the pressure range of 5−7 Torr and at 298 ± 2 K. The reaction product, the NO_3−isoprene adduct radical, was directly detected using the CIMS method. In addition, density functional theory and ab initio molecular orbital calculations have been employed to determine the structures and energies of the NO_3−isoprene adduct isomers. Geometry optimizations were performed using density functional theory at the B3LYP/6-31G(d,p) level, and the single-point energies were computed using second-order Møller−Plesset perturbation theory and the coupled-cluster theory with single and double excitations including perturbative corrections for the triple excitations (CCSD(T)). At the CCSD(T)/6-31G(d) level of theory, the zero-point-corrected energies of the NO_3−isoprene adduct radicals are 15 to 31 kcal mol^{-1} more stable than the separated NO_3 and isoprene, and the isomers of terminal NO_3 additions are more energetically favorable than those of internal NO_3 additions. The rate constants of the formation of the NO_3−isoprene adduct radicals and their isomeric branching have been calculated using the canonical variational transition state theory.

Introduction

Photochemical oxidation of atmospheric volatile organic compounds (VOCs) results in ozone and secondary organic aerosol formation, with major implications for local and regional air quality and global environmental changes.[1] Isoprene (2-methyl-1,3-butadiene, $CH_2{=}C(CH_3)CH{=}CH_2$) is one of the most abundant hydrocarbons naturally emitted by the terrestrial biosphere, with a global averaged production rate of about 450 Tg $year^{-1}$.[2] Because of its high chemical reactivity and proliferation in the generation of organic peroxy radicals, isoprene plays an important role in ozone formation in local and regional atmosphere.[3,4] Atmospheric oxidation of isoprene is initiated by reactions with a variety of oxidant species. Because isoprene is mainly produced in the daytime, the reaction with hydroxyl radial OH is the dominant tropospheric removal pathway. Reactions of isoprene with ozone, nitrate radical NO_3, and halogen atoms and their oxides can also be important and may in some cases give a larger contribution to the oxidation rate than OH. The nitrate radical, which is formed by the reaction of NO_2 and ozone, is a major tropospheric nighttime oxidant. The nighttime reaction between isoprene and nitrate radicals contributes significantly to the degradation of isoprene, which also exists with a considerable amount at night.[5,6]

The initial reaction between isoprene and NO_3 proceeds mainly by NO_3 addition to the >C=C< double bond,[7] forming the NO_3−isoprene adduct radical, the nitrooxyalkyl radical

$$NO_3 + C_5H_8 \rightarrow C_5H_8NO_3^{\bullet} \quad (1)$$

Under atmospheric conditions, the nitrooxyalkyl radical is expected to react primarily with oxygen molecules to form the nitrooxyalkyl peroxy radicals

$$C_5H_8NO_3^{\bullet} + O_2 \rightarrow C_5H_8NO_3O_2^{\bullet} \quad (2)$$

Addition of O_2 occurs only at the carbons β to the NO_3 position for the NO_3−isoprene adducts of internal NO_3 addition but takes places at two centers (β or δ to the NO_3 position) for the NO_3−isoprene adducts of terminal NO_3 addition. Hence, O_2 addition to the NO_3−isoprene adduct leads to the formation of four β- and two δ-nitrooxyalkyl peroxy radicals. The nitrooxyalkyle peroxy radical can further react with NO to form six (β or δ) nitrooxyalkoxy radicals, engage in a self-reaction or reaction with other peroxy radicals, or undergo isomerization or decomposition, leading to various oxygenated or nitrated organic species. Hence, the organic intermediate radicals play a key role of propagation or termination of the oxidation process. In particular, the isomeric branching of the initial NO_3 addition to isoprene is crucial in determining the final product distribution. Figure 1 shows a mechanistic diagram for the initial reaction of isoprene with NO_3 to form the nitrooxyalkyl radical.

Several laboratory studies have investigated the kinetics and mechanism of the oxidation reactions of isoprene initiated by NO_3. The rate constant between isoprene and NO_3 has been studied using both a relative rate method[8−10] and absolute rate measurements.[11−13] Currently, there is a disagreement in the reported rate constants among the various studies, with values ranging from 5.9×10^{-13} to 13.0×10^{-13} cm^3 $molecule^{-1}$ s^{-1} in the pressure range of 0.4−760 Torr. Experimental studies have also been carried out to identify the reaction products,[10,14,15] which provide insight about the reaction mechanism. On the basis of an environmental chamber study of the NO_3-isprene

* To whom correspondence should be addressed.

10.1021/jp0105950 CCC: $20.00
Published on Web 05/30/2001

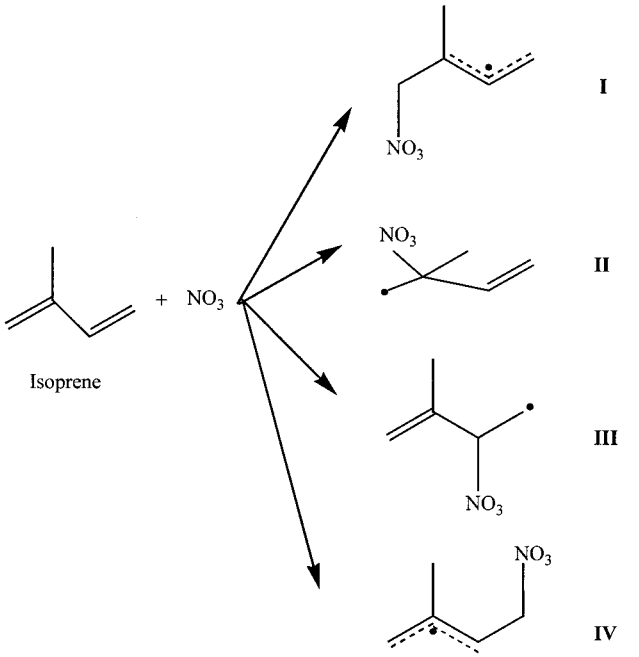

Figure 1. Mechanistic diagram for the addition reaction of NO_3 to isoprene.

reactions using FTIR spectroscopy, Skov et al.[14] reported insignificant yields for unsubstituted carbonyl compounds but found 3-methyl-4-nitoxy-2-butenal as the dominate product. Their study using isoprene and isoprene-4,4-d_2 suggested that NO_3 addition to the C1-position dominates over addition to the C4-position, with a branching ratio of 3.5 between the two channels. Another study, using a flow system in conjunction with GC−MS/FID, direct MS, and long path FTIR detection, has also reported the products from the NO_3−isoprene reactions.[10] Berndt and Boge[10] provided evidence for the pressure-dependent formation of two oxiranes, 2-methyl-2-vinyl-oxirane and 2-(1-methyl-vinyl)-oxirane, which are derivatives from decomposition of the vibrationally excited nitrooxyalkyl radicals of terminal NO_3 additions at C1- and C4-positions, respectively. The authors also suggested that in the presence of O_2 molecules the final product distribution is strongly dependent on the reaction pathways of the peroxy radicals formed. If the peroxy radicals mainly react in a self-reaction, the formation of 3-methyl-4-nitoxy-2-butenal is dominant. In the presence of NO, the peroxy radicals mainly react with NO to form the nitrooxyalkoxy radicals, which further decompose to form methyl vinyl ketone (MVK), along with minor 3-methylfuran (MF) and methacrolein (MACR). On the basis of a ratio of the yields of MVK and MACR, Berndt and Boge[10] reported a branching ratio of 5.1−7.4 between NO_3 additions to C1 and C4 additions, in disagreement with the value reported by Skov et al.[14] In addition, using atmospheric pressure ionization tandem mass spectrometry (API−MS/MS), Kwok et al. observed the formation of several nitrooxycarbonyls, hydroxynitrates, nitrooxyhydroperoxides, and hydroxycarbonyls.[15]

In this study, we report laboratory and theoretical studies of the reaction of isoprene with NO_3. The rate constant of the reaction of NO_3 with isoprene has been measured in the pressure range of 5−7 Torr and at the temperature of 298 ± 2 K. Using the CIMS method, we are able to directly detect the nitrooxyalkyl radicals. In addition, we report density functional theory (DFT) and ab initio calculations of the nitrooxyalkyl radical. The geometries and energetics of the four isomers of the NO_3−isoprene adduct radicals are presented. We have calculated the rate constants and isomeric branching of the formation of the nitrooxyalkyl radicals, using the presently obtained ab initio results and canonical variational transition state theory (CVTST).

Experimental Section

A fast-flow reactor, in conjunction with chemical ionization mass spectrometry (CIMS) detection, was used in the present experiments. The experimental setup is similar to that used by us previously, and detailed descriptions of the experimental apparatus have been given elsewhere.[16,17] Briefly, it consists of a flow reactor of 1.78 cm i.d. and 120 cm in length. All surfaces exposed to the reactants and products were coated with a halocarbon wax. A flow of He carrier gas (in the range of 1−3 STP l min^{-1}) was injected to the flow reactor through an entrance port in the rear of the flow reactor. The pressure of the flow reactor was regulated between 5 and 7 Torr, and the temperature of the flow reactor was maintained at 298 ± 2 K. Typical flow velocity in the flow reactor ranged from 1300−2500 cm s^{-1}. Isoprene was added to the flow reactor through a series of five addition ports located 5 cm apart at the downstream end of the flow tube. The flow reactor was operated under the laminar flow condition with Reynolds number $Re = 2au\rho/\mu'$ typically in the range of 10−30, where a is the internal radius of the flow reactor, ρ is the density of the gas, u is the flow velocity, and μ' is the viscosity coefficient of the gas. Under our experimental conditions, a laminar flow was fully developed, and homogeneous mixing of both NO_3 and isoprene was effectively achieved.[16]

Reactants and products of the NO_3−isoprene reaction were detected by CIMS using either positive or negative reagent ions. The CIMS employed a new approach, involving an electrostatic ion guide recently developed.[18,19] Positive or negative reagent ions were initiated using corona discharge at a high voltage (−5 kV). The SF_6^- reagent ions were generated by adding a small amount of SF_6 to a He carrier flow (about 1−2 slpm at STP) through the discharge. The positive reagent ions O_2^+ were produced by passing the He carrier flow through the discharge and then adding a small amount of O_2 downstream. An electrostatic ion guide was used to transport ions to the quadrupole mass analyzer. The use of the ion guide allows for both ion transportation with a high efficiency and preferential separation and removal of neutral molecules in a differential pumping system.[18,19]

The NO_3 radical was generated by thermal decomposition of N_2O_5 at a temperature of 400 K according to $N_2O_5 + He \rightarrow NO_2 + NO_3 + He$ ($k \approx 50$ s^{-1}).[20] N_2O_5 was synthesized by reacting O_3 with NO_2 in an oxygen carrier at room temperature and further distilled at 195 K. Care was taken to remove impurities such as NO_2 and HNO_3 because of their possible interference with the detection of the nitrate radical. O_3 was prepared by flowing molecular oxygen through an ozonizer. The purity of the N_2O_5 sample was verified to be greater than 95% using FTIR spectroscopy and mass spectrometry. N_2O_5 was introduced to the flow reactor by passing a small He flow through the N_2O_5 trap held at 195 K and was detected using I^- reagent ion, formed by electron attachment to CF_3I.[21,22] The nitrate radical was detected according to the ion−molecule reaction $NO_3 + SF_6^- \rightarrow NO_3^- + SF_6$. The ion−molecule rate constant of this reaction has not been measured, but it is exothermic because the electron affinity of NO_3 (3.94 eV)[23] is larger than that of SF_6 (1.05 eV).[24] The NO_3 concentration in the flow tube was estimated using two methods. First, the NO_3 concentration was determined relative to NO_2 by converting NO_3 to NO_2 according to the reaction $NO_3 + NO \rightarrow 2NO_2$ ($k = 1.1$

$\times 10^{-11} \exp\{-(170 \pm 100)\}/T)$ cm^3 molecule^{-1} s^{-1})[20] in excess of NO. Alternatively, we measured the enhancement of the NO_2 signal when N_2O_5 was introduced into the system. Typically, the concentration of nitrate radicals in the flow reactor was estimated in the range of $4-9 \times 10^{10}$ molecule cm^{-3}.

Commercially available isoprene (Aldrich 99.5%) was used to volumetrically prepare a 1% to 5% isoprene/He mixture in a 2 L glass bulb, which was then introduced to the flow reactor using a 10 sccm flow meter. The concentrations of isoprene in the flow reactor were regulated in the range of $1-9 \times 10^{13}$ molecule cm^{-3}, so that the [isoprene]/[NO_3] ratio was at least a factor of 100 to ensure the pseudo-first-order kinetic assumption. Isoprene was detected by the CIMS using positive reagent ions at its parent ion peak. For both NO_3 and isoprene the mass spectrometer signals were linear over the range of the concentrations used.

Theoretical

The theoretical computations were performed on an SGI Origin 2000 supercomputer using the Gaussian 98 software package.[25] All radicals were treated with the unrestricted Hartree−Fock (UHF) formulation. Geometry optimization was executed using Becke's three parameter hybrid method employing the LYP correction function (B3LYP) in conjunction with the split valence polarized basis set 6-31G(d,p). The DFT structures were then employed in single-point energy calculations using frozen-core second−order Møller−Plesset perturbation theory (MP2) and coupled-cluster theory with single and double excitations including perturbative corrections for the triple excitations (CCSD(T)) with various basis sets. Harmonic vibrational frequency calculations were made using B3LYP/6-31G(d,p).

Recently, we have investigated analogous reactions of OH and Cl additions to isoprenet.[26,27] Those studies indicate that the calculated energetics are very sensitive to effects of basis set and electron correlation. For the nitrooxyalkyl radicals, single-point energy calculations at the CCSD(T) level of theory using a larger basis set (e.g., 6-311++G(d,p)) are extremely computationally demanding. We have corrected basis set effects on the calculated energies for the isomers of the nitrooxyalkyl radicals, on the basis of an approach that has been recently developed and employed to investigate the energetics for the OH-isoprene adduct isomers.[26] The procedure involves determination of a correction factor associated with basis set effects at the MP2 level and subsequent correction to the energy calculated at a higher level of electron correlation with a moderate size basis set. For the isomers of the nitrooxyalkyl radicals, the basis set effects on the energies were evaluated at the MP2 level. A correction factor, CF, was determined from the energy difference between the MP2/6-31G(d) and MP2/6-311++G(d,p) levels. The values of calculated energies at the CCSD(T)/6-31G(d) level were then corrected by the MP2 level correction factors.

Results and Discussions

Measurements of the Rate Constant of the Isoprene Reaction with NO_3. Measurements of the bimolecular rate constant for the reaction of isoprene with NO_3 were performed under the pseudo-first-order condition, using isoprene as the excess reagent. The kinetics of the reaction were obtained by monitoring the disappearance of NO_3. The decay of the NO_3 signal as a function of the reaction distance was used to derive the observed first-order loss rate coefficient (k^I, s^{-1}). Figure 2 shows the decay of NO_3 in the presence of isoprene. The experiment was performed at 5.6 Torr, with $Re = 12$. From Figure 2, the observed first-order rate coefficients (k^I) were determined from the slopes of plots of the logarithm of NO_3 signal vs the injector distance and from the flow velocity. In our experiments, there was a background signal at mass 62, most likely from the presence of HNO_3 and N_2O_5 in the flow tube, because both species react efficiently with SF_6^- to produce NO_3^-.[21,22] The possible contribution of HNO_3 and N_2O_5 to the signal at mass 62 was assessed by reacting NO_3 to completion (>99.9%) with an excess of isoprene, so that the signal at mass 62 became invariant when the distance to introduce isoprene was varied. The background signal at mass 62 was subtracted from all of the data in the kinetic analysis. We determined that the heterogeneous loss of NO_3 on the wall of the reactor was small, generally less than 1 s^{-1}. The effects of axial and radial diffusions of the reactants were estimated using the approach described by Brown.[28] Using the appropriate gas-phase diffusion coefficient for NO_3, the correction because of gas-phase diffusion in the axial and radial directions was estimated to be less than 3%. This correction was smaller than the random and systematical errors estimated in our experiments. Hence, we have neglected the gas-phase diffusion correction and obtained the bimolecular rate constant directly from the observed first-order loss coefficient for NO_3.

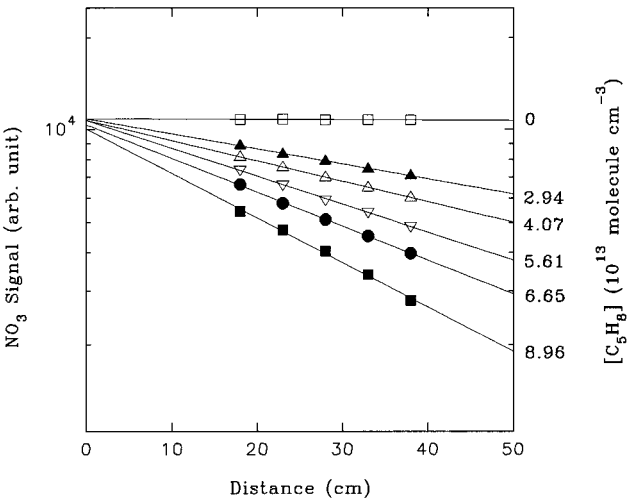

Figure 2. Decay of NO_3 signal as a function of injector distance at various concentrations of isoprene. Experimental conditions are $P =$ 5.6 Torr, $U = 1916$ cm s^{-1}, and $Re = 12$.

The first-order rate coefficients were plotted against the isoprene concentration in Figure 3. The slope of the fit provides an effective bimolecular rate constant for the reaction between isoprene and NO_3, corresponding to a value of 7.3×10^{-13} cm^3 molecule^{-1} s^{-1}. Similar measurements were performed in the pressure range of 5−7 Torr, and the results are summarized in Table 1. Our averaged rate constant over the pressure range of 5−7 Torr is $(7.3 \pm 0.2) \times 10^{-13}$ cm^3 molecule^{-1} s^{-1}. The uncertainty represents the scatter in the data at the 1 standard deviation level and is not an estimate of systematic errors. We estimate that systematic uncertainty in our measured rate constants is within ±10%, considering the possible sources of error in the measurements (i.e., gas flows, temperature, detection signal, and pressure) and in the flow considerations. Table 2 compares our measured rate constant with those previously reported. The literature rate constants vary within a factor of 2 in the pressure range from 0.4−760 Torr. A value of 6.8×10^{-13} cm^3 molecule^{-1} s^{-1} has been recommended for modeling this reaction in the atmosphere.[2] Our measured rate is about 7% higher than the currently recommended value.

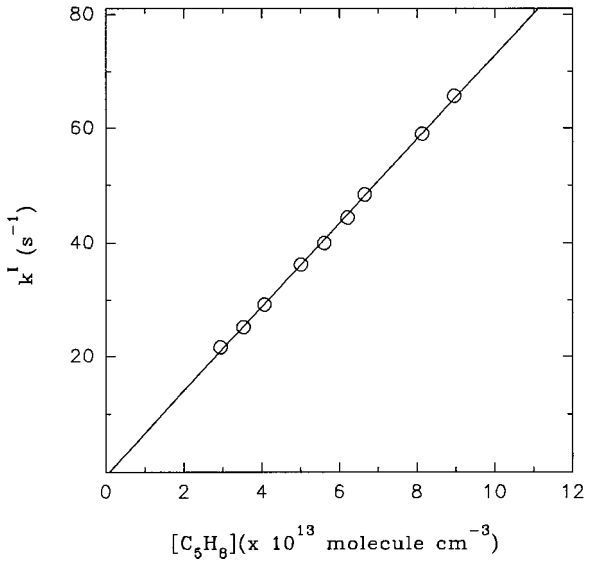

Figure 3. First-order loss rate coefficient k^I as a function of isoprene concentration. Experimental conditions are similar to those in Figure 2.

TABLE 1: Results of Rate Constant Measurements for the Reaction between Isoprene and NO_3 at 298 ± 2 K[a]

exp. no.	pressure (Torr)	flow velocity (cm s^{-1})	rate constant (10^{-13} cm^3 $molecule^{-1}$ s^{-1})
1	5.4	2263	7.1
2	6.0	2204	7.4
3	5.3	2267	7.3
4	5.1	2184	7.3
5	5.2	1985	7.2
6	5.2	2215	7.6
7	5.6	1916	7.3
ave			7.3 ± 0.2

[a] The initial concentration ranges are $[NO_3]_o$ = (4−9) × 10^{10} molecule cm^{-3} and $[C_5H_8]_o$ = (1−9) × 10^{13} molecule cm^{-3}.

TABLE 2: Summary of Measured Rate Constants for the Reaction of NO_3 with Isoprene

k (10^{-13} cm^3 $molecule^{-1}$ s^{-1})	T (K)	P (Torr)	technique[a]	ref
5.9 ± 0.7	298	735	SC−R	8
13.0 ± 1.4	298		FT−MS	11
6.5 ± 0.8	297	1.0 to 1.1	FT−LIF	12
12.1 ± 2.0	298 ± 2	760	SC−R	9
7.8 ± 0.6	298	0.7 to 3.0	FT−MS	13
6.9 ± 2.6	298	5 to 75	FT−R	10
7.3 ± 0.2	298	5 to 7	FT−CIMS	this work

[a] SC, smog chamber; R, relative method; FT, flow tube; MS, mass spectrometry; and LIF, laser induced fluorescence.

Observation of the NO_3−Isoprene Adduct. Using the CIMS method, we were able to directly monitor the product of the reaction of isoprene with NO_3, the NO_3−isoprene adduct radical. This adduct can be detected with O_2^+ reagent ions according to the following ion−molecule reaction

$$O_2^+ + C_5H_8NO_3^\bullet \rightarrow C_5H_8NO_3^+ + O_2 \qquad (3)$$

An analogous detection scheme has been used to detect other adduct radicals from the Cl-initiated reaction of isoprene and OH-initiated reactions of isoprene and toluene.[16,29,30] As is shown in Figure 1, the addition of NO_3 to the double bonds of isoprene results in the formation of four possible isomeric adduct radicals. The mass spectrometer is sensitive only to the mass of ions that are detected and does not discriminate between isomers.

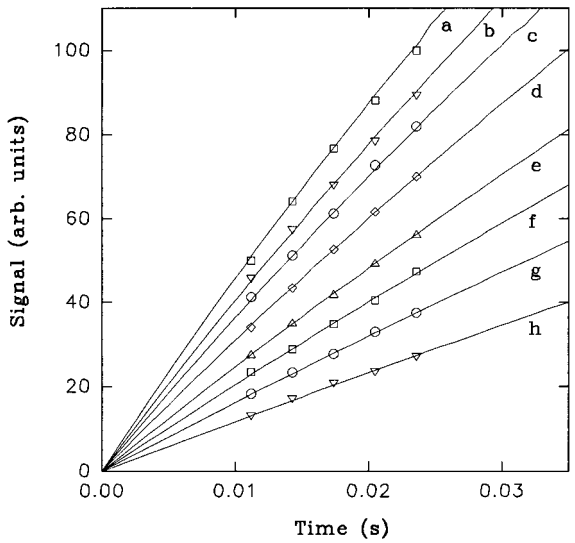

Figure 4. Variation of NO_3−isoprene adduct signals as a function of reaction time. The solid curves are based on a kinetic simulation (see text). Experimental conditions are P = 7.0 Torr, U = 1611 cm s^{-1}, Re = 13, and $[C_5H_8]_o$ = (a) 13.1, (b) 11.5, (c) 10.3, (d) 8.7, (e) 6.9, (f) 5.7, (g) 4.5, and (h) 3.3 × 10^{12} molecule cm^{-3}.

Several procedures were taken to positively verify that the ions detected at m/e = 130 were indeed attributable to the NO_3−isoprene adduct, rather than from secondary ion−molecule reactions. First, we observed that the signal at mass 130 disappeared when either the isoprene flow was stopped or when the heater for dissociating N_2O_5 was turned off. Those steps were necessary to ensure that this mass peak was related to the presence of isoprene or NO_3 radicals in the flow reactor. Alternatively, we monitored the 130 mass peak when the reaction time was successively increased. Figure 4 shows an example of the NO_3−isoprene adduct formation at various isoprene concentrations. As is shown in this figure, there is a gradual increase in the NO_3−isoprene adduct signal when the reaction distance is increased and the adduct signal intensifies at a higher isoprene concentration. The curves are fitted through the experimental data using a kinetic program.[16,29,30] The model input included the initial concentrations of NO_3, isoprene, and all other precursors. The reaction system considered in the simulation included the NO_3−isoprene reaction, along with other related secondary reactions. Under our experimental conditions, the reverse reaction of NO_2 and NO_3 to form N_2O_5 was not important. In addition, we did not include the decomposition of the adduct isomers, on the basis of our theoretical prediction to be discussed below. A rate constant of 7.3 × 10^{-13} cm^3 $molecule^{-1}$ s^{-1} for the NO_3−isoprene reaction was used in fitting all of the data in Figure 4. Because of the relatively slow rate of the reaction of isoprene with NO_3, fitting to experimental data was sensitive to the rate constant of the NO_3−isoprene reaction within 30% at the highest isoprene concentration (curve a) and within a factor of 2 at the lowest isoprene concentration (curve h) for the 95% confidence level.

Structures and Energetics of NO_3−Isoprene Adduct Isomers. DFT and ab initio molecular orbital calculations were performed to obtain the structures and energetics of the nitrooxyalkyl radicals. Geometry optimization of the isomers of the nitrooxyalkyl radicals was performed at the B3LYP/6-31G(d,p) level of theory. For each isomer, we explored the possible rotational conformers to locate the energy minimum, including cis and trans configurations. A total of more than 40 rotational conformers were considered for the NO_3−isoprene adduct, but we report only the global rotational minima for each

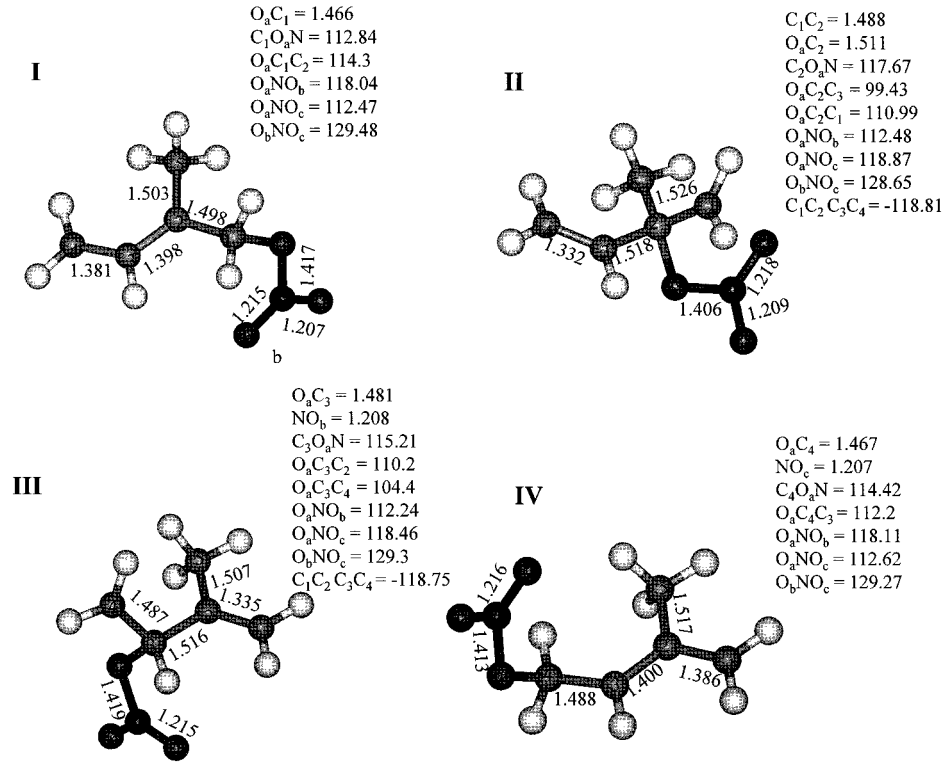

Figure 5. Optimized geometries of the four isomers of the nitrooxyalkyl radicals calculated at the B3LYP/6-31G(d,p) level of theory (bond lengths in angstroms and angles in degrees).

TABLE 3: Calculated Total Energies (in hartrees) and Spin Eigenvalues for the NO_3−Isoprene Adduct Radicals

isomer	B3LYP/ 6-31G(d,p)	MP2/ 6-31G(d)	MP2/ 6-311++G(d,p)	CCSD(T)/ 6-31G(d)	S^2(B3LYP)
I	−475.586875	−474.148851	−474.429302	−474.256125	0.7785
II	−475.552593	−474.126045	−474.408674	−474.228255	0.7549
III	−475.557585	−474.132535	−474.415408	−474.232589	0.7538
IV	−475.584043	−474.146066	−474.426409	−474.253441	0.7799
NO_3	−280.216801	−279.459187	−279.607123	−279.526253	0.7547
C_5H_8	−195.322536	−194.593517	−194.727793	−194.672991	0

family of the structural isomers. The geometries of the lowest energy conformers were confirmed as minima on the potential surfaces by frequency calculations performed at the B3LYP/6-31G(d,p) level. The energy differences among the rotational conformers were typically within 3.0 kcal mol^{-1}, much smaller than those of the distinct structural isomers.

The geometries of the lowest energy rotational conformers for the four isomers of the NO_3−isoprene adduct are illustrated in Figure 5. For radicals **I** and **IV**, the C−C bond lengths between carbons two and three are very similar, with values of 1.389 and 1.400 Å, respectively. The C−C double bond lengths between carbons three and four in radical **I** (1.381 Å) and between carbons one and two in radical **IV** (1.386 Å) also closely resemble the bond lengths between carbons two and three of the two radicals. These bond lengths are between the typical values for a σ bond and Π bond, indicating significant Π bonding character. Hence, the two isomers with NO_3 addition to the terminal positions (**I** and **IV**) contain delocalized double bonds in a resonance structure between the three terminal carbons, reflecting the allylic nature of both radicals. For radicals **II** and **III**, the C−C single bond lengths between carbons two and three are 1.518 and 1.516 Å, noticeably larger than the corresponding values of radicals **I** and **IV**. However, the lengths of the terminal C−C double bond between carbons three and four in radical **II** (1.332 Å) and between carbon one and three in radical **III** are comparable to the corresponding bonds in radicals **I** and **IV**, showing significant Π bonding character. For radicals **II** and **III**, the bonding characteristic of the terminal carbon pair (i.e., carbons three and four in **II** and one and two in **III**) is not significantly affected by the NO_3 addition. Both radicals contain well-localized double bonds, and the unpaired electron is located at the terminal carbon adjacent to the point of addition. In addition, the O−C bond lengths for radicals **I** and **IV** (1.466 and 1.467 Å) are somewhat shorter than those of radicals **II** and **III** (1.511 and 1.481 Å).

A comparison of the structures of the four lowest energy isomers of the NO_3−isoprene adduct to those of the OH−isoprene adduct recently investigated[25] exhibits some similarity. For example, except for the O−C bond distance, the C−C bond lengths of the corresponding isomers of the NO_3−isoprene and OH−isoprene adducts are very similar. In both cases, the isomers with the terminal addition have a shorter C−O bond length than that of the internal addition.

The total energies of the nitrooxyalkyl radicals were determined with the B3LYP/6-31G(d,p) optimized geometries using MP2 and CCSD(T) with different basis sets. The results of the total energies are summarized in Table 3. Also included in Table 3 for comparison are the calculated total energies for isoprene and NO_3. For the nitrate radical, our calculated equilibrium structures are consistent with those reported previously.[30,31] Spin contamination associated with the B3LYP optimized geometries of the four adduct radical isomers is minimal. The calculated

TABLE 4: Zero-Point Corrected Relative Energies (RE) (kcal mol^{-1}) and Heats of Formation (ΔH_f^0; kcal mol^{-1}) for the NO_3−Isoprene Radicals

	RE					ΔH_f^0
isomer	B3LYP/ 6-31G(d,p)	MP2/ 6-31G(d)	MP2/ 6-311++G(d,p)	CCSD(T)/ 6-31G(d)	CCSD(T)/ 6-31G(d)+*CF*	CCSD(T)/ 6-31G(d)+*CF*
I	0	0	0	0	0	4.96
II	20.21	13.00	11.64	16.18	14.82	19.78
III	17.08	8.94	7.42	13.47	11.95	16.91
IV	1.89	1.86	1.93	1.80	1.86	6.83

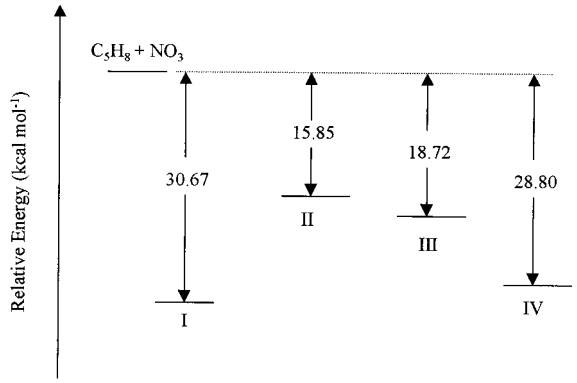

Figure 6. Energy level of the isomers of the nitrooxyalkyl radicals relative to NO_3 and isoprene obtained at the CCSD(T)/6-31G(d) + CF// B3LYP/6-31G(d,p) level of theory.

spin eigenvalues, $\langle S^{**}2\rangle$, are 0.779 and 0.780 for radicals **I** and **IV**, respectively, and are even lower for radicals **II** and **III** (0.755 and 0.754). After the S + 1 component is annihilated, the values of $\langle S^{**}2\rangle$ are reduced to 0.750 for all four isomers (which is identical to the exact value of a pure doublet), indicating that contamination of the unrestricted Hartree−Fock wave function from higher spin states is negligible for the four adduct radicals.

Results of the computed relative energies of the four isomers of the NO_3−isoprene adduct are listed in Table 4. Table 4 reveals that the calculated related energies are sensitive to both electron correlation and basis set effects. For isomers **II** and **III**, the relative energies calculated using CCSD(T) are higher than those calculated using MP2 with the same basis set (6-31G(d)) but are lower than those determined using B3LYP. Using MP2, the relative energy differences between basis 6-31G(d) and 6-311++G(d,p) are 1.4 and 1.5 kcal mol^{-1} for radicals **II** and **III**, respectively. Correction for the basis set factors slightly reduces the relative energies obtained using CCSD(T). As is seen from Table 4, isomer **I** has the lowest energy and isomer **IV** has the second lowest energy (by about 1.8 kcal mol^{-1} more than **I**), whereas isomers **II** and **III** have much higher energies. Hence, the single-point energy calculations at all levels of theory produce consistent results: the terminal additions of NO_3 to isoprene are energetically more favorable than the additions to the internal positions. The relative energetic stability of the NO_3−isoprene adduct isomers is insensitive to electron correlation effects. Figure 6 shows a schematic of the potential energy surface for the NO_3−isoprene reaction, obtained at the CCSD(T)/6-31G(d) + CF level of theory. The NO_3−isoprene adduct radicals are 15−31 kcal mol^{-1} more stable than the separated NO_3 and isoprene, with the binding energies 30.7, 15.9, 18.7, and 28.8 kcal mol^{-1} for isomers **I**−**IV,** respectively. We estimate an uncertainty of ±2 kcal mol^{-1} associated with the energetics of the nitrooxyalkyl radical, on the basis of a validation study of similar radical species.[26]

Also included in Table 4 are the standard heats of formation for the lowest energy isomers, estimated from the calculated total energy (E), the experimentally known heats of formation for the reactants, and thermal energy (TE) correction obtained from the frequency calculations. The single-point energies of all of the reactants and products were computed at the CCSD-(T)/6-31G(d) + CF//B3LYP/6-31G(d,p) level and the thermal energy (TE) correction through frequency calculations at the B3LYP/6-31G(d,p)//B3LYP/6-31G(d,p) level. The heat of reaction (ΔE) for the addition reaction of NO_3 to isoprene is expressed by

$$\Delta E = [E(\text{adduct}) - E(\text{isoprene}) - E(NO_3)] + [\text{TE(adduct)} - \text{TE(isoprene)} - \text{TE}(NO_3)] \quad (4)$$

Alternatively, the heat of reaction for the reaction of NO_3 with isoprene is given as

$$\Delta E = \Delta H_f^0(\text{adduct}) - \Delta H_f^0(\text{isoprene}) - \Delta H_f^0(NO_3) \quad (5)$$

where ΔH_f^0(isoprene) and $\Delta H_f^0(NO_3)$ are the heats of formation for isoprene and NO_3, respectively. For the NO_3 radical, the previously reported heat of formation is 17.6 ± 1.0 kcal mol^{-1}.[10,26,32] The heats of formation for the four adduct isomers were calculated by equating the above two equations, with values of 5.0, 20.0, 17.0, and 6.8 kcal mol^{-1} for isomers **I**−**IV**, respectively.

Rate Constant Calculations. The high-pressure rate constants for the formation of the nitrooxyalkyl radicals were calculated using canonical variational transition state theory (CVTST). Recently this approach has been employed to determine the rate constants of OH addition to isoprene and O_2 addition to the OH−isoprene adduct.[33,34] The association rate is related to the dissociation rate by

$$\frac{k_{rec}}{k_{uni}} = \frac{Q_{AB}}{Q_A Q_B} \exp\left(\frac{\Delta E'}{kT}\right) \quad (6)$$

where Q_{AB} is the partition function of the adduct, Q_A and Q_B are the partition functions of the individual reactants, and $\Delta E'$ is zero-point corrected reaction energy. The unimolecular rate is expressed by

$$k_{uni} = \frac{kT}{h} \frac{Q_{AB}^{\ddagger}}{Q_{AB}} \exp\left(-\frac{\Delta E}{kT}\right) \quad (7)$$

where $Q_{AB}^{\ddagger}$ is the partition function of the transition state with the vibrational frequency corresponding to the reaction coordinate removed, Q_{AB} is the partition function of the adduct, and ΔE is the zero-point corrected transition state energy relative to the separated reactants.

The partition functions for eqs 6 and 7 were calculated by treating the rotational and translational motion classically and treating vibrational modes quantum mechanically. Unscaled

vibrational frequencies and moments of inertia for the NO_3−isoprene adducts were taken from the calculations at the B3LYP/6-31G(d,p) level. The reaction and activation energies (i.e., $\Delta E'$ and ΔE) were taken to be zero-point corrected energies calculated at the CCSD(T)/6-31G(d) + CF// B3LYP/6-31G(d,p) level. The conserved modes of the transition state were assumed to resemble the product modes. The dependence of the transitional mode frequencies with C−O distance were modeled using[35]

$$\nu(r) = \nu_0 \exp[-a(r - r_e)] + B \qquad (8)$$

where υ_0 is the vibrational frequency in the reactant molecule, r_e is the equilibrium bond distance, B is the sum of the rotational constants of the individual isoprene and NO_3 molecules, and a is a constant. Moments of inertia at fixed geometries were calculated by changing only the C−O distance. The potential energy surface along the reaction coordinate was modeled by a Morse function including the centrifugal barrier

$$V(r) = D_e[1 - \exp(-\beta r)]^2 + B_{ext}(r)J(J+1) \qquad (9)$$

where D_e is the bond dissociation energy, $B_{ext}(r)$ is the external rotational constant determined by assuming that the molecular was a symmetric top, and J was assumed to be the average rotational quantum number of a Boltzmann distribution calculated using the external rotational constant of the molecule at the equilibrium configuration. The individual rates of formation of each isomer were obtained using eqs 6 and 7, variationally minimizing the rate as function of the C−O bond distance.

We performed additional DFT calculations to identify the nature of the potential along the reaction coordinate for NO_3 addition to isoprene, specifically to determine whether there is a well-defined transition state or the addition proceeds without a barrier via a loose transition state. For isomers **I** and **IV**, we employed a constrained optimization procedure for geometry optimization at fixed C−O bond lengths using B3LYP/6-31G(d) (for isomer **I** and **IV**) and B3LYP/6-31G(d,p) (for isomer **I**). The C−O bond length was increased successively from −0.3 up to 3.0 Å relative to the equilibrium C−O bond length of the corresponding radical, with an interval of 0.2 Å. We find that no energy exceeds the bond dissociation energy along the reaction coordinate and that the Morse potential derived from eq 9 provides a reasonable functional form to model the reaction coordinate. The β parameter for the Morse potential in eq 9 is given by $\beta = (2\pi^2\mu/D_e)^{1/2}$, where μ is the reduced mass of the bonded atoms, D_e is the bond dissociation energy, and υ is the vibrational frequency of the reaction coordinate in the parent molecule.[36] The individual β parameters used in the rate calculations for the four isomers were derived using the CCSD(T)/6-31G(d) + CF binding energies for each species. The value of a was estimated to be 1.40 $Å^{-1}$ by summing the individual association rate rates until the overall rate was equivalent to our measured value. The results of the calculated rate constants are shown in Table 5 for each adduct isomer. The high-pressure rate constants are in the range of 3×10^{-15}−6×10^{-13} cm^3 $molecule^{-1}$ s^{-1}. The dissociation rates of the adduct isomers are small, less than 500 s^{-1} for isomers **II** and **III** and 10^{-5} s^{-1} for **I** and **IV**. It is evident from Table 5 that the addition rates to form isomers **I** and **IV** are significantly higher than those to form radicals **II** and **III**. On the basis of the CVTST calculations, we determine the relative branching ratios of 0.835:0.005:0.010:0.150 for isomers **I**−**IV**, respectively. Note that the calculated branching ratios and rate constants of the nitrooxyalkyl radicals are strongly dependent on the nature of the transition states.[37,38] We estimated an uncertainty of 10% in our predicted branching ratios.

TABLE 5: CVTST Calculated High-Pressure Rate Constants for the NO_3−Isoprene Adduct Radical Formation[a]

isomer	rate of formation (cm^3 $molecules^{-1}$ s^{-1})	branching ratio
I	6.0×10^{-13}	0.835
II	3.7×10^{-15}	0.005
III	6.9×10^{-15}	0.010
IV	1.1×10^{-13}	0.150
total	7.2×10^{-13}	1.00

[a] See text for details.

The CVTST calculations predict a strong preference for isomer **I**, which is in agreement with the previous product studies.[10,14] Skov et al.[14] evaluated the branching ratio for the formation of the two allylic radicals after the initial attack of NO_3 in positions one and four using d_2-isoprene, CH_2=$C(CH_3)$−CH=CD_2. The authors obtained a ratio of 3.5 between the rates of the two pathways, based on a ratio of the intensities of the $-CH_2ONO_2$ and $-CD_2ONO_2$ groups, whose spectral features are located at 1282 and 1300 cm^{-1}, respectively. In addition, they found 3-methyl-4-nitoxy-2-butenal as the dominate product, which is formed from subsequent reactions of the peroxy radical with C1 (NO_3) and C4 (O_2) additions. Berndt and Boge[10] reported observation of two oxiranes, 2-methyl-2-vinyl-oxirane and 2-(1-methyl-vinyl)-oxirane, which are formed from decomposition of the vibrationally excited nitrooxyalkyl radicals of terminal NO_3 additions at C1 and C4 positions, respectively. The formation yields of the two oxirances were found to be dependent on pressure, with an averaged ratio of 5.34 ± 1.02. In the presence of NO, the authors found dominant formation of MVK, along with minor MF and MACR. Using the ratio of MVK and MACR yields, Berndt and Boge[10] estimated a branching ratio of 5.1−7.4 between NO_3 additions to C1 and C4 additions, somewhat larger than the value reported by Skov et al.[14] Hence, the earlier product studies have clearly demonstrated the preferential addition of NO_3 addition to C1 than to C4 position, consistent with the theoretical prediction based on the CVTST calculations.

Conclusions

We have presented experimental and theoretical studies of the reaction of isoprene with NO_3. The rate constant of the reaction of isoprene with NO_3 has been measured in the pressure range of 5−7 Torr and at 298 ± 2 K. Direct observation of the NO_3−isoprene adduct has been made using the CIMS method. DFT and ab initio molecular orbital calculations have been performed to investigate the structures and energetics the nitrooxyalkyl radical. At the CCSD(T)/6-31G(d) level of theory, the zero-point-corrected energies of the NO_3−isoprene adduct radicals are 15−31 kcal mol^{-1} more stable than those of the separated NO_3 and isoprene. We found no evidence for an energetic barrier for NO_3 addition to isoprene, and the ab initio results have been employed to determine the formation rates of the NO_3−adduct radicals using canonical variational transition state theory (CVTST). The calculated isomeric branching suggests preferential addition of NO_3 to C1 position, consistent with previous product studies of the NO_3−isoprene reaction system.

Acknowledgment. This work was supported by a grant from the Robert A. Welch Foundation (A-1417). Additional support for the computation part of this research was provided by the

Texas A&M University Supercomputing Facilities. We are grateful to S. North and L. Thompson for helpful discussions and acknowledge the use of the Laboratory for Molecular Simulations at Texas A&M.

References and Notes

(1) Seinfeld, J. H.; Pandis, S. N. *Atmospheric Chemsitry and Physics: From Air Pollution to Climate Change*; John Wiley & Sons: New York, 1997.
(2) Rasmussen, R. A.; Khalil, M. A. *J. Geophys. Res.* **1988**, 93, 1477.
(3) Trainer, M.; et al. *Nature* **1987**, *329*, 705.
(4) Chameides, W. L.; Lindsay, R. W.; Richardson, J.; Kiang, C. S. *Science* **1988**, *241*, 1473.
(5) Riemer, D. D.; Milne, P. J.; Farmer, C. T.; Zika, R. G. *Chemosphere* **1994**, *28*, 837.
(6) Starn, T. K.; Shepson, P. B.; Bertman, S. B.; Riemer, D. D.; Zika, R. G.; Olszyna, K. *Geophys. Res. Lett.* **1998**, *103*, 22437.
(7) Atkinson, R. *J. Phys. Chem. Ref. Data Monogr*. **1994**, *2*, 1.
(8) Atkinson, R.; Aschmann, S. M.; Winer, A. M.; Pitts, J. N. *Environ. Sci. Technol*. **1984**, *18*, 370.
(9) Barnes, I.; Bastian, V.; Becker, K. H.; Tong, Z. *J. Phys. Chem.* **1990**, *94*, 2413.
(10) Berndt, T.; Boge, O. *Int. J. Chem. Kinet.* **1997**, *29*, 755.
(11) Benter, Th.; Schindler, R. N. *Chem. Phys. Lett.* **1988**, *145*, 67.
(12) Dlugokencky, E. J.; Howard, C. J. *J. Phys. Chem.* **1989**, *93*, 1091.
(13) Wille, U.; Becker, E.; Schindler, R. N.; Lancar, I. T.; Poulet, G.; Le Bras, G. *J. Atmos. Chem.* **1991**, *13*, 183.
(14) Skov, H.; Hjorth, J.; Lohse, C.; Jensen, N. R.; Restelli, G. *Atmos. Environ.* **1992**, *26A*, 2771.
(15) Kwok, E. S. C.; Ashmann, S. M.; Arey, J.; Atkinson, R. *Int. J. Chem. Kinet.* **1996**, *28*, 925.
(16) Suh, I.; Zhang, R. *J. Phys. Chem. A* **2000**, *104*, 6594.
(17) Zhang, R.; Suh, I.; Clinkenbeard, A.; Lei, W.; North, S. W. *J. Geophys. Res.* **2000**, *105*, 24627.
(18) Zhang, R.; Molina, L. T.; Molina, M. J. *Rev. Sci. Instrum.* **1998**, *69*, 4002.
(19) Zhang, R.; Lei, W.; Molina, L. T.; Molina, M. J. *Int. J. Mass Spectrom. Ion Proc*. **2000**, *194*, 41.
(20) DeMore, W. B.; Sander, S. P.; Howard, C. J.; Ravishankara, A. R.; Golden, D. M.; Kolb, C. E.; Hampson, R. F.; Kurylo, M. J.; Molina, M. J. *Chemical Kinetics and Photochemical Data for Use in Stratospheric Modeling: JPL Publication 97-4*; NASA: Linthicum Heights, MD, 1997.
(21) Zhang, R.; Leu, M. T.; Keyser, L. F. *Geophys. Res. Lett.* **1995**, *22*, 1493.
(22) Zhang, R.; Leu, M. T.; Keyser, L. F. *J. Geophys. Res.* **1995**, *100*, 18845.
(23) Weaver, A.; Arnold, D. W.; Bradforth, S. E.; Neumark, D. M. *J. Chem. Phys.* **1991**, *94*, 1740.
(24) Streit, G. E. *J. Chem. Phys.* **1982**, *77*, 826.
(25) Frisch, M. J.; Trucks, G. W.; Schlegel, H. B.; Scuseria, G. E.; Robb, M. A.; Cheeseman, J. R.; Zakrzewski, V. G.; Montgomery, J. A., Jr.; Stratmann, R. E.; Burant, J. C.; Dapprich, S.; Millam, J. M.; Daniels, A. D.; Kudin, K. N.; Strain, M. C.; Farkas, O.; Tomasi, J.; Barone, V.; Cossi, M.; Cammi, R.; Mennucci, B.; Pomelli, C.; Adamo, C.; Clifford, S.; Ochterski, J.; Petersson, G. A.; Ayala, P. Y.; Cui, Q.; Morokuma, K.; Malick, D. K.; Rabuck, A. D.; Raghavachari, K.; Foresman, J. B.; Cioslowski, J.; Ortiz, J. V.; Stefanov, B. B.; Liu, G.; Liashenko, A.; Piskorz, P.; Komaromi, I.; Gomperts, R.; Martin, R. L.; Fox, D. J.; Keith, T.; Al-Laham, M. A.; Peng, C. Y.; Nanayakkara, A.; Gonzalez, C.; Challacombe, M.; Gill, P. M. W.; Johnson, B. G.; Chen, W.; Wong, M. W.; Andres, J. L.; Head-Gordon, M.; Replogle, E. S.; Pople, J. A. *Gaussian 98*, revision D.3; Gaussian, Inc.: Pittsburgh, PA, 1998.
(26) Lei, W.; Derecskei-Kovacs, A.; Zhang, R. *J. Chem. Phys.* **2000**, 113, 5354.
(27) Lei, W.; Zhang, R. *J. Chem. Phys.* **2000**, *113*, 153.
(28) Brown, R. L. *J. Res. Natl. Bur. Stand. (U.S.)* **1978**, *83*, 1.
(29) Zhang, R.; Lei, W. *J. Chem. Phys.* **2000**, *113*, 8574.
(30) Molina, M. J.; Zhang, R.; Broekhuizen, K.; Lei, W.; Navarro, R.; Molina, L. T. *J. Am. Chem. Soc*. **1999**, *121* (43), 10225.
(31) Morris, V. R.; Bhatia, S. C.; Hall, J. H., Jr. *J. Phys. Chem.* **1990**, *94*, 7414.
(32) Morris, V. R.; Bhatia, S. C.; Hall, J. H., Jr. *J. Phys. Chem.* **1991**, *95*, 9203.
(33) Burrows, J. P.; Tyndall, G. S.; Moortgat, G. K. *Chem. Phys. Lett.* **1985**, *119*, 193.
(34) Lei, W.; Zhang, R.; McGivern, W. S.; Derecskei-Kovacs, A.; North, S. W. *Chem. Phys. Lett.* **2000**, *326*, 109.
(35) Lei, W.; Zhang, R.; McGivern, W. S.; Derecskei-Kovacs, A.; North, S. W. *J. Phys. Chem.* **2001**, *105*, 471.
(36) Hase, W. L. *Chem. Phys. Lett.* **1987**, *139*, 389.
(37) Gilbert, R. G.; Smith, S. C *Theory of Unimolecular and Recombination Reaction*s; Blackwell Scientific: Oxford, U.K., 1990.
(38) Holbrook, K. A.; Pilling, M. J.; Robertson, S. H. *Unimolecular reactions*; John Wiley & Sons: New York, 1996.